

Facies changes and a major negative $\delta^{13}\text{C}$ shift suggest the base of Mila Formation as the likely base of the Miaolingian Series, Alborz Mountains, northern Iran

Hadi Amin-Rasouli¹ and Yaghoob Lasemi^{2,*}

¹Department of Geosciences, University of Kurdistan, Sanandaj, Iran

²Illinois State Geological Survey, University of Illinois at Urbana-Champaign, Champaign, Illinois, USA

INTRODUCTION

The Cambrian System in the Alborz Mountains of northern Iran (Fig. 1A) consists of alternating carbonate and siliciclastic successions deposited in an extensive platform covering the length of the Cimmerian and the Arabian-Iranian plates in northeast Gondwana (e.g., Berberian and King, 1981, Lasemi, 2001). In Alborz, the lower–middle Cambrian transition (Fig. 1B) includes the siliciclastic Top Quartzite of the Lalun Formation (Assereto, 2014) and the chiefly carbonate deposits of Member 1 of the Mila Formation (Stöcklin et al., 1964). We have not applied the stratigraphic nomenclature by Geyer et al. (2014) because their approach has several shortcomings (see Lasemi and Amin-Rasouli, 2017, p. 344–345 and discussions therein). The lower–middle Cambrian transition in northern Iran is plagued by the absence of biostratigraphic criteria; here, we integrate sequence stratigraphy with $\delta^{13}\text{C}$ composition to evaluate the base of the Cambrian third series, the Miaolingian Series, in northern Iran. Our objective is to provide a valuable non-biostratigraphic criteria in the Alborz to permit chronostratigraphic correlation of this interval with other regions. This study provides evidence for the terminal early Cambrian extinction event and the resulting paleoenvironmental changes during the middle Cambrian in northern Iran.

METHODS

A composite section for the east-central Alborz Mountains comprising the Top Quartzite in the Tuyeh section and the lower part of the Mila Formation in the Shahmirzad section is placed in a sequence stratigraphic framework (Fig. 2A). For carbon isotope analysis, avoiding weathered/calcite filled cavities, 11 carbonate samples were collected to cover the basal 9 m of the Mila Formation. Because of sanctions, politico-economic reasons, and lack of funding only the basal part of Mila was sampled. Sample powders were analyzed for carbon and oxygen isotopes at the Stable Isotope

Laboratory of the Institute for Geology, Leibniz University Hannover, Germany. The sample aliquots were reacted with 100% phosphoric acid at 72°C in a Thermo-Finnigan GasBench II. The produced CO_2 was transferred into a Thermo-Finnigan Delta-V advantage mass spectrometer. Repeated analysis of NBS 19, NBS 18, IAEA CO-1, and Lausan certified in-house carbonate standards produced an external reproducibility of $\leq 0.05\text{‰}$ and $\leq 0.06\text{‰}$ for $\delta^{13}\text{C}$ and $\delta^{18}\text{O}$, respectively. Results are in per mil (‰) relative to the conventional V-PDB.

STRATIGRAPHIC VARIABILITY AND $\delta^{13}\text{C}$ ANALYSIS

The lower–middle Cambrian transition encompasses two depositional sequences (Fig. 2A). The Top Quartzite sequence records deposition in a shoreface system and conformably overlies the Shale unit of the Lalun Formation. Its transgressive and early highstand packages consist of interbedded gray shale and quartzose sandstone (Fig. 1C). The late highstand package is a thickening upward cross-bedded to planar-bedded upper shoreface sandstone that unconformably underlies the Mila Formation (Fig. 1D, E). The basal Mila sequence is a shallow marine succession and comprises a transgressive package (2.5 m) the lower part of which (~70 cm) is characterized by varicolored calcareous mudstone and/or argillaceous limestone/dolostone tidal rhythmites (Fig. 1D) grading upward to distal open marine thin-bedded, dark gray rhythmic shale and micritic limestone (Fig. 1E). This interval thickens upward in the early highstand package and grades to dolostone containing a thrombolite reef zone (~3 m) in which domical bioherms become larger upward (Fig. 1e) and encompass well-preserved clotted fabric (Fig. 2B). The early highstand package underlies the unconformity capped late highstand ramp margin ooid grainstone and peritidal facies (Fig. 2A).

Carbonate carbon isotopic analysis records a large-magnitude negative $\delta^{13}\text{C}$ shift (-3.86‰) in the lowest sampled layer ~70 cm above the base of the Mila Formation. The $\delta^{13}\text{C}$ values increase upward to -0.05‰ in the upper part of the thrombolite reef zone and change to $+0.31\text{‰}$ in the ooid grainstone bed at about 9 m from the base of

Copyright © 2021 by the SEPM Society for Sedimentary Geology
doi: 10.2110/sedred.2021.1.04
Manuscript submitted: 09/10/2020
Received in revised format: 02/23/2021
Manuscript accepted: 02/24/2021

*Corresponding author: ylasemi@illinois.edu

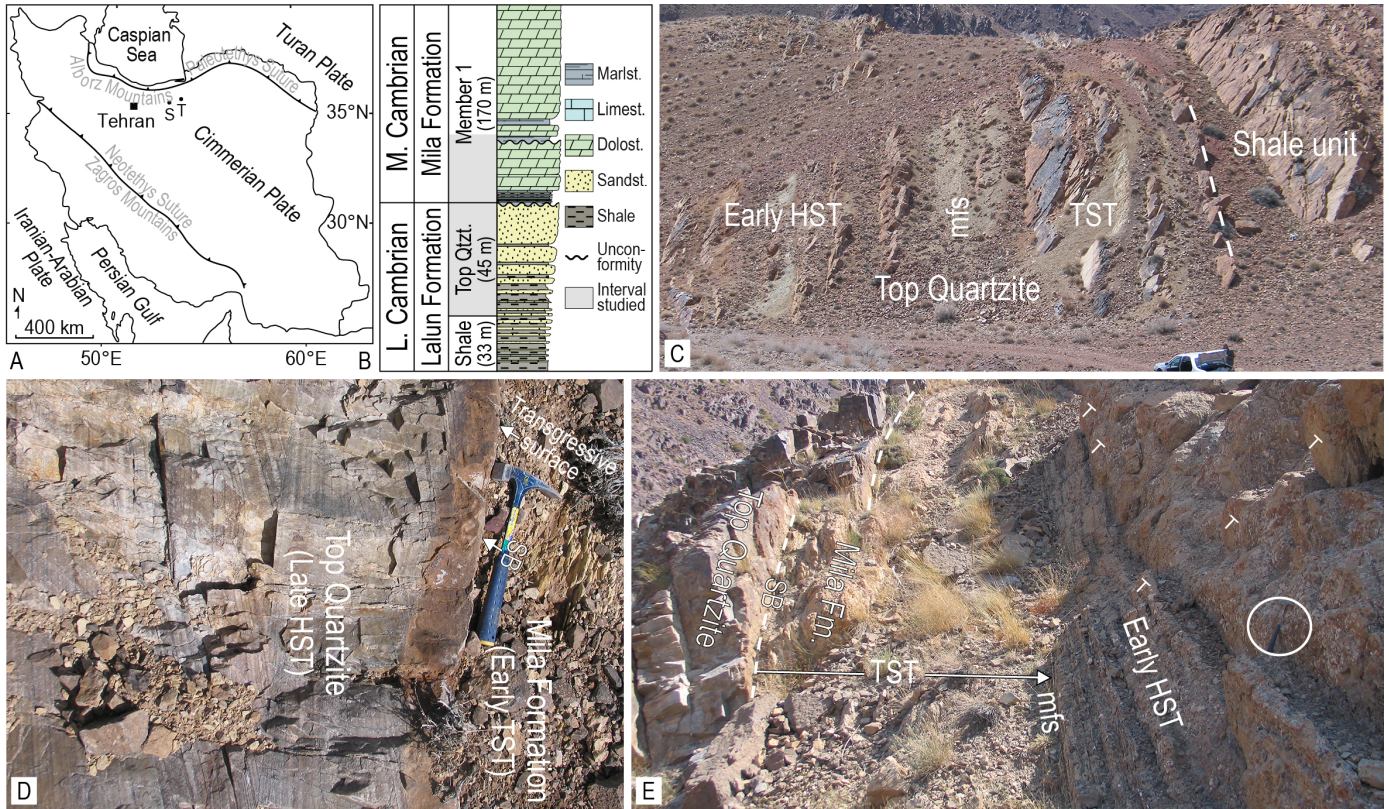


Figure 1: (A) Map of Iran showing tectonic plates and the location of Shahmirzad (S) and Tuyeh (T) sections (from [Lasemi and Amin-Rasouli, 2017](#)). (B) Stratigraphic nomenclature and composite section of the lower–middle Cambrian transition comprising the upper part of the Shale unit and the Top Quartzite unit of Lalun in Tuyeh and Member 1 of the Mila Formation in Shahmirzad. (C) The lower portion of the Lalun Top Quartzite sequence that conformably overlies the Shale unit (Tuyeh section, stratigraphic top to the left and view to the southeast). Note that sandstone layers thin upward in the TST but thicken upward in the early HST. (D) The unconformity capped Top Quartzite late highstand package that underlies the tidal rhythmites of the lowermost transgressive package of the basal Mila sequence. (E) The upper part of the Top Quartzite that unconformably underlies the lower part of the basal Mila sequence (Shahmirzad section, view to the NE and stratigraphic top to the right). Note very thin-bedded rhythmic shale and micritic limestone that thickens upward in the early highstand package containing thrombolite bioherms (T). Abbreviations: HST: Highstand systems tract; mfs: Maximum flooding surface; SB: Sequence boundary; TST: Transgressive systems tract.

Mila Formation (Fig. 2A). Field and petrographic studies indicate that influence of diagenesis was minimal because the sampled dense micritic limestone and dolostone could inhibit movement of diagenetic fluids. Lack of correlation between carbon and oxygen isotope values (Fig. 2C) suggests the primary carbon isotope signature of original seawater (e.g., [Azmy et al., 2014](#)). Furthermore, unlike the $\delta^{18}\text{O}$, influence of diagenesis and burial temperature on $\delta^{13}\text{C}$ values of carbonates is insignificant (e.g., [Swart, 2015](#)).

DISCUSSION AND CONCLUSIONS

The terminal early Cambrian in Laurentia and south China is marked by the mass extinction of trilobites associated with a large-magnitude negative carbon isotope excursion (e.g., [Lin et al., 2019](#)). [Montañez et al. \(2000\)](#) first reported a major short-term (~ 100 k.y.) negative $\delta^{13}\text{C}$ shift ($\geq 4\text{‰}$) in the terminal early Cambrian in Laurentia, just prior to the extinction of olenellid trilobites. A rather large negative $\delta^{13}\text{C}$ shift is also recognized at the base of the middle Cambrian boundary in south China preceding the extinction

level of Redlichiid trilobites, the base of the recently defined Miaolingian Series ([Zhao et al., 2019](#)). [Zhu et al. \(2006\)](#) named the foregoing exertions Redlichiid Olenellid Extinction Carbon Isotope Excursion (ROECE). Recent studies, however, have questioned the ROECE definition documenting that the extinction level of olenellids and redlichiids and their associated $\delta^{13}\text{C}$ excursions, here referred to as “RECE” and “OECE” (Fig. 2D), are not synchronous ([Lin et al., 2019](#), [Geyer, 2019](#), [Sundberg et al., 2020](#)).

The major negative $\delta^{13}\text{C}$ shift ~ 70 cm above the base of Mila unconformable boundary, like south China (e.g., [Zhao et al., 2019](#)), occurs within the transgressive phase of a major global eustatic event and likely corresponds to the “RECE” excursion (Fig. 2D) and may define the Series 2-Miaolingian boundary in northern Iran. The Mila thrombolites (Fig. 2A, B), like the basal Famennian (e.g., [Whalen et al., 2002](#)) and the basal Triassic (e.g., [Kershaw et al., 2012](#)), appear in a very short stratigraphic interval close to the unconformity and could represent a post-extinction boundary thrombolite. As the consequence of post-extinction

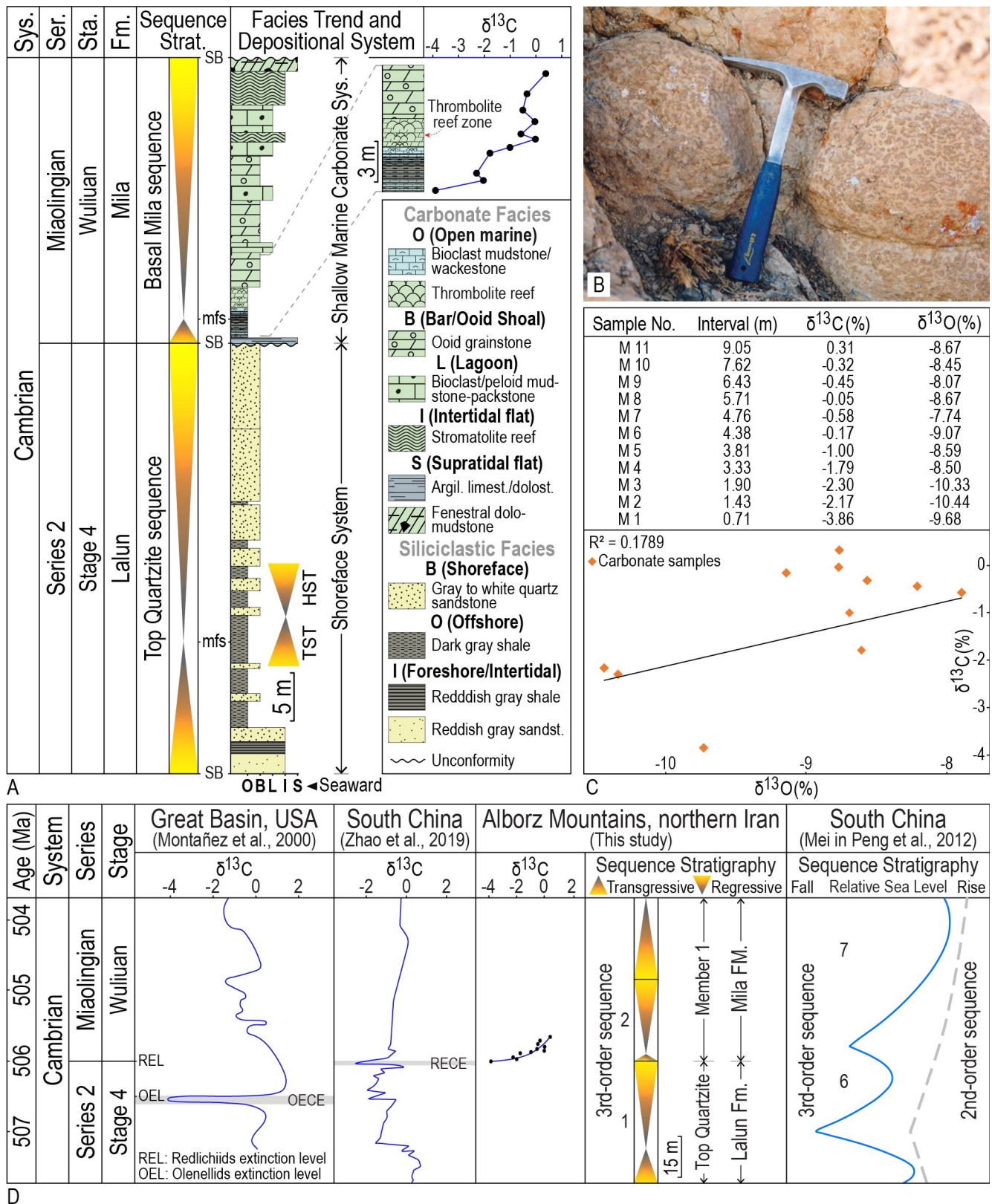


Figure 2: (A) Vertical facies trend and $\delta^{13}\text{C}$ composition of the Series 2-Miaolingian transition comprising the Top Quartzite and the basal Mila sequences in the Tuyeh and Shahmirzad composite section. (B) Close up view of domal thrombolite bioherms in Fig. 1E showing clotted fabric (from Lasemi and Amin-Rasouli, 2017). (C) Geochemical data and $\delta^{18}\text{O}$ vs $\delta^{13}\text{C}$ crossplot. (D) Correlation of the base of Mila $\delta^{13}\text{C}$ shift with those in Laurentia and south China, as well as correlation of the 3rd-order sequences in the Alborz with the sequences recorded at the Series 2-Miaolingian transition in south China (time scale and extinction level after Sundberg et al., 2020).

environmental stress and metazoan reef crisis (e.g., [Mata and Bottjer, 2012](#)) owing to sea level rise and low marine oxygenation ([Lee and Riding, 2018](#)), the middle Cambrian rocks in Iran are microbial carbonates dominated by stromatolites, oncoids, and ooids (e.g., [Lasemi, 2001](#)). The lower–middle Cambrian transition in northern Iran records a major transformation in depositional regime from the regressive Top Quartzite siliciclastics to the transgressive base of Mila carbonates. The Top Quartzite and the basal Mila sequences (sequences 1 and 2), using the current time scale ([Sundberg et al., 2020](#)), correlate with the south China third-order sequences (sequences 6 and 7 of [Mei et al., 2007](#) in [Peng et al., 2012](#)) at the Series 2-Miaolingian transition (Fig. 2D). Results of this study suggest that the base of the Miaolingian is likely to be placed at the base of Mila Formation in northern Iran. Future work should test this interpretation by focusing on facies and carbon isotope studies covering the entire middle–upper Cambrian succession.

ACKNOWLEDGMENTS

We thank Jeong-Hyun Lee, the editor of SEPM's *The Sedimentary Record* and two anonymous reviewers for their thoughtful comments and suggestions. We are grateful to Ulrich Heimhofer from the Institute for Geology, Leibniz University Hannover, Germany for providing the opportunity for isotope analysis; many thanks go to Amin Navidtalab for his assistance with this analysis.

Literature Cited

- Assereto, R. (2014). The Paleozoic formations in central Alborz, Iran. *Rivista Italiana di Paleontologiae Stratigrafia*, 69:503–543.
- Azmy, K., Stouge, S., Brand, U., Bagnoli, G., and Ripperdan, R. (2014). High-resolution chemostratigraphy of the Cambrian–Ordovician GSSP: Enhanced global correlation tool. *Palaeogeography, Palaeoclimatology, Palaeoecology*, 409:135–144.
- Berberian, M. and King, G. C. P. (1981). Towards a paleogeography and tectonic evolution of Iran. *Canadian Journal of Earth Sciences*, 18(2):210–265.
- Geyer, G. (2019). A comprehensive Cambrian correlation chart. *Episodes*, 42(4):321–332.
- Geyer, G., Bayet-Goll, A., Wilmsen, M., Mahboubi, A., and Moussavi-Harami, R. (2014). Lithostratigraphic revision of the middle Cambrian (Series 3) and upper Cambrian (Furongian) in northern and central Iran. *Newsletter on Stratigraphy*, 47:21–59.
- Kershaw, S., Crasquin, S., Li, Y., Collin, P.-Y., Forel, M.-B., Mu, X., Baud, A., Wang, Y., Xie, S., Maurer, F., and Guo, L. (2012). Microbialites and global environmental change across the Permian–Triassic boundary: A synthesis. *Geobiology*, 10(1):25–47.
- Lasemi, Y. (2001). *Facies Analysis, Depositional Environments and Sequence Stratigraphy of the Upper Pre-Cambrian and Paleozoic Rocks of Iran*. Geological Survey of Iran. 180 p. (in Persian).
- Lasemi, Y. and Amin-Rasouli, H. (2017). The lower–middle Cambrian transition and the Sauk I–II unconformable boundary in Iran, a record of late early Cambrian global Hawke Bay regression. In Sorkhabi R., editor, *Tectonic Evolution, Collision, and Seismicity of Southwest Asia: In Honor of Manuel Berberian's Forty-Five Years of Research Contributions*, volume 525 of *Geological Society of America Special Papers*, pages 153–171.
- Lee, J.-H. and Riding, R. (2018). Marine oxygenation, lithistid sponges, and the early history of Paleozoic skeletal reefs. *Earth-Science Reviews*, 181:98–121.
- Lin, J.-P., Sundberg, F. A., Jiang, G., Montañez, I. P., and Wotte, T. (2019). Chemostratigraphic correlations across the first major trilobite extinction and faunal turnovers between Laurentia and South China. *Scientific Reports*, 9(1):1–15.
- Mata, S. A. and Bottjer, D. J. (2012). Microbes and mass extinctions: Paleoenvironmental distribution of microbialites during times of biotic crisis. *Geobiology*, 10(1):3–24.
- Mei, M. X., Zang, C., Zang, H., Meng, X. Q., and Chen, Y. H. (2007). Sequence-stratigraphic frameworks for the Cambrian of the Upper-Yangtze Region: Ponder on the forming background of the Cambrian biological diversity events. *Journal of Stratigraphy*, 31:68–78.
- Montañez, I. P., Osleger, D. A., Banner, J. L., Mack, L. E., and Musgrove, M. (2000). Evolution of the Sr and C isotope composition of Cambrian oceans. *GSA Today*, 10(5):1–7.
- Peng, S., Babcock, L. E., and Cooper, R. A. (2012). The Cambrian Period. In Gradstein, F. M., Ogg, J. G., Schmitz, M. D., and Ogg, G. M., editors, *The Geologic Time Scale, 2nd edition*, pages 437–488.
- Stöcklin, J., Ruttner, A. W., and Nabavi, M. H. (1964). *New data on the lower Paleozoic and pre-Cambrian of north Iran*. Geological Survey of Iran, Report 1, 29 p.
- Sundberg, F. A., Karlstrom, K. E., Geyer, G., Foster, J. R., Hagadorn, J. W., Mohr, M. T., Schmitz, M. D., Dehler, C. M., and Crossey, L. J. (2020). Asynchronous trilobite extinctions at the early to middle Cambrian transition. *Geology*, 48(5):441–445.
- Swart, P. K. (2015). The geochemistry of carbonate diagenesis: The past, present and future. *Sedimentology*, 62(5):1233–1304.
- Whalen, M. T., Day, J., Eberli, G. P., and Homewood, P. W. (2002). Microbial carbonates as indicators of environmental change and biotic crises in carbonate systems: Examples from the Late Devonian, Alberta basin, Canada. *Palaeogeography, Palaeoclimatology, Palaeoecology*, 181(1-3):127–151.
- Zhao, Y., Yuan, J., Babcock, L. E., Guo, Q., Peng, J., Yin, L., Yang, X., Peng, S., Wang, C., Gaines, R. R., Esteve, J., Tai, T., Yang, R., Wang, Y., Sun, H., and Yang, Y. (2019). Global standard Stratotype-section and point (GSSP) for the conterminous base of the Miaolingian series and Wuliuan stage (Cambrian) at Balang, Jianhe, Guizhou, China. *Episodes*, 42(2):165–183.
- Zhu, M.-Y., Babcock, L. E., and Peng, S.-C. (2006). Advances in Cambrian stratigraphy and paleontology: Integrating correlation techniques, paleobiology, taphonomy and paleoenvironmental reconstruction. *Palaeoworld*, 15(3-4):217–222.